CALCIUM SULFATE SCALING DELAY TIMES UNDER SENSIBLE HEATING CONDITIONS

F. Fahiminia, A.P. Watkinson and N. Epstein

Department of Chemical and Biological Engineering
The University of British Columbia, 2360 East Mall, Vancouver, BC, Canada, V6T 1Z3

ABSTRACT

Crystallization of calcium sulfate, an inverse solubility salt, on a heated surface under sensible heating conditions has been studied. A temperature measurement technique was employed to detect delay times. Experiments were carried out to determine how process variables such as surface and bulk temperature, concentration, and velocity affect the delay times of calcium sulfate scaling. Analysis of the results yields values of calcium sulfate surface energies and the delay time activation energies under different operating conditions, and a comparison between them and the values reported by other researchers in the literature is made.

INTRODUCTION

Calcium sulfate scaling can give rise to operating problems and additional costs in industrial systems and desalination units. In order to control scale formation it is desirable to understand the mechanisms of its inception. Initiation is the first step of the successive events that commonly occur in crystallization fouling (Epstein, 1983), and it is important to quantify the relationship between the relevant variables in this step. In general, initiation is associated with the delay time, the period of time that elapses between the achievement of supersaturation and the first detection of a fouling deposit. The duration of the delay time for a given system is affected by the degree of supersaturation, the temperature level, the fluid velocity and the presence of impurities. The occurrence of a delay time is undoubtedly related to the kinetics of nucleation, but its duration is difficult to predict. It has been shown that $CaSO_4$ nucleation on the heat transfer surface of a non-boiling flow exchanger is a transient nucleation phenomenon (Hasson and Zahavi, 1970). Also, Branch (1991) correlated the reciprocal of the delay time as if it were independent of solute concentration but with an Arrhenius dependence on wall temperature, but Najibi et al. (1997) showed that the delay time is a strong function of the degree of supersaturation and, therefore, cannot be expressed by a zero-order model.

Classical nucleation theory (Mullin, 2001) provides a basis for delay time studies. According to the nucleation theory, delay time is a function of temperature, supersaturation ratio, and surface energy. In this study, the delay time nucleation theory model is used to analyze the experimental results and generate values of surface energies under different operating conditions.

EXPERIMENTAL

The apparatus, illustrated in Figure 1, consists of a flow loop in which the calcium sulfate solution is continuously recirculated from a holding tank through a 1-μm filter, the heated test section, a series of double pipe coolers and back to the holding tank. The test section is constructed of drawn T304 stainless steel (ASTM A269-80A) tube with a length of 1.83 m, an outside diameter of 9.525 mm, a wall thickness of 0.254 mm and a heated length of 0.771 m, which is subjected to electrical resistance heating at a constant and uniform heat flux. The bulk inlet and outlet temperatures were measured by thermocouples. The bulk inlet temperature was maintained constant during each experiment (covering a range of 45 to 65˚C for all of the experiments), while clean tube surface temperatures were varied from 73 to 83˚C, as measured by ten thermocouples spaced longitudinally on the outside of the test section as illustrated in Figure 2 and Table 2. The

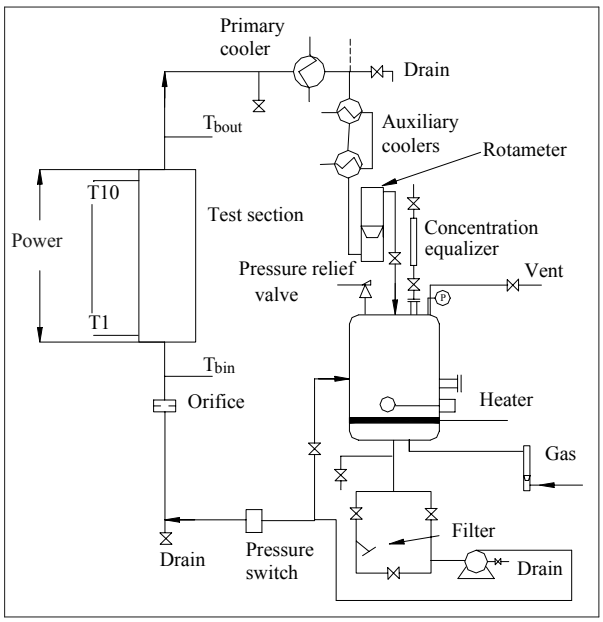

Figure 1. Schematic of the Tube Fouling Unit (TFU)

rate of rise in surface temperature gives a measure of the local fouling resistance at that temperature. This Tube Fouling Unit (TFU) (Wilson and Watkinson, 1996; Rose et al., 2000) is configured such that test sections are used only once, and then sectioned to allow in situ deposit examination and further analysis of the nature of the deposit material, either by optical microscopy, scanning electron microscopy, elemental analysis or deposit coverage studies. A concentration equalizer (installed on top of the holding tank) was employed to keep concentration constant during each experiment. It can be isolated from the rest of the apparatus, which is running at high pressure during the experiment, using a connective valve and then, after adding the required chemicals to the equalizer, the valve is opened gradually to let chemicals flow into the holding tank while the pressure is kept constant.

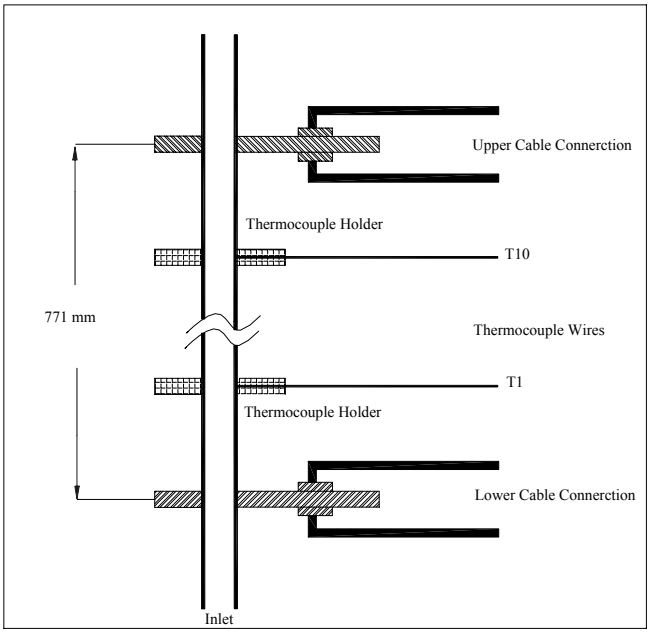

Figure 2. Schematic of the test section construction

Due to the longitudinal temperature gradient at the surface of the tube, the highest rates of fouling occurred at the locations of the highest temperature thermocouples, and thus limited the duration of an experiment. Because clean surface temperatures were as high as 83˚C, it was necessary to maintain some over-pressure (typically about 80 psig) on the test section to prevent the onset of boiling as the surface temperature rose due to fouling. Because of the high temperature limitation, some of the thermocouples from the low temperature regions of the tube gave barely measurable delay times. Reynolds numbers based on local fluid properties were varied from 3000 to 37000 to provide adequate data for a study of the velocity effect on the delay times.

Batches of calcium sulfate solution were prepared by dissolving calcium nitrate, Ca $(NO_3)_2 \cdot 4H_2O$, and sodium sulfate, Na_2SO_4, in distilled water. After ensuring the required concentration level by using EDTA titration, the solution was added to the holding tank. Prior to the addition of heat to the test section, the solution was circulated for one hour to ensure a thoroughly well mixed chemical system. The power to the test section was then applied to achieve the operating conditions required. Heating up the test section to steady state took approximately 30 minutes.

SURFACE ENERGY

Surface nucleation is the prerequisite for crystal growth on the surface, and therefore, the presence of the first seeds or nuclei plays an important role. Although it is difficult to have purely surface nucleation, i.e. without some accompanying nucleation away from the surface, experiments were carried out under conditions (low bulk temperature and high surface temperature accompanied by eliminating particles using a 1-μm filter) in which it is believed that crystal initiation was dominated by surface nucleation.

Based on classical nucleation theory (Mullin, 2001), the rate of homogeneous nucleation, J, i.e. the number of nuclei formed per unit time per unit surface area can be expressed as:

$$J = A\exp\left[-\frac{\beta\gamma^3 v_m^2}{N_A^2 n^2 k_B{}^3 T^3 (\ln S)^2}\right] \quad (1)$$

where A is a frequency factor, β is a shape factor ($=16\pi/3$), γ is the crystal surface energy, v_m is the molar volume of the crystalline phase (7.445×10^{-5} m^3/mol for $CaSO_4 \cdot 2H_2O$), N_A is Avogadro's number (6.022×10^{23} mol^{-1}), n is the number of ions of a crystallizing salt molecule ($n = 2$ for $CaSO_4 \cdot 2H_2O$), k_B is the Boltzmann constant (1.38×10^{-23} J/K), T is the absolute temperature (K), and S is the supersaturation ratio (C/C_s), where C and C_s are solution and saturation concentrations, respectively. Eq. (1) indicates that three main variables govern the rate of nucleation: temperature, T; degree of supersaturation, S; and surface energy, γ. A model can be developed by assuming that the induction time τ_D is inversely proportional to the nucleation rate (Mullin, 2001):

$$\tau_D = \frac{B}{J} \quad (2)$$

Combining Eqs. (1) and (2), we arrive at:

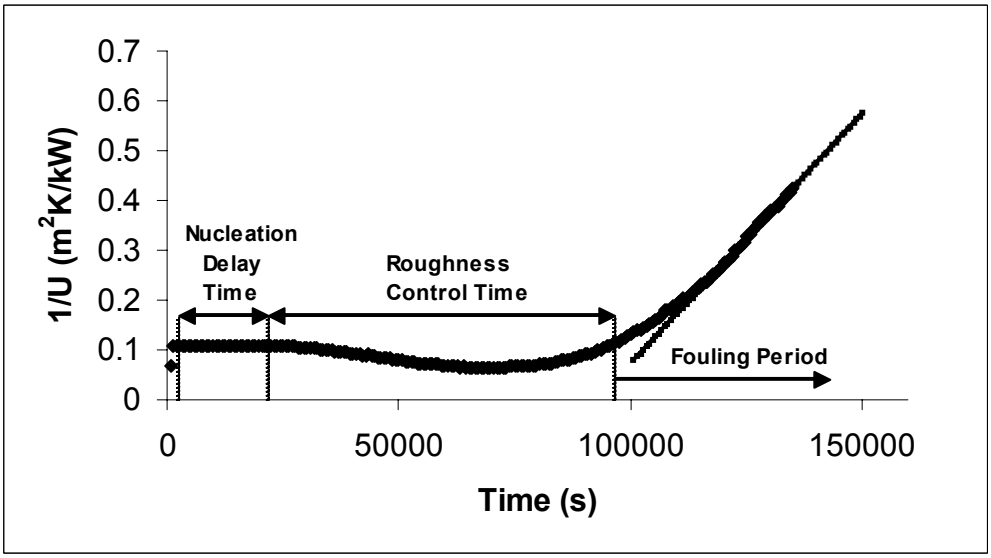

Figure 3. Reciprocal local heat transfer coefficient (V = 1.2 m/s, $T_{w,c}$ = 82˚C, T_b = 62˚C, C = 3128 ppm, Z = 716 mm)

$$\ln \tau_D = \ln \frac{B}{A} + \frac{K}{(\ln S)^2} \quad (3)$$

where

$$K = \frac{\beta \gamma_{eff}^{\ 3} \nu_m^{\ 2}}{N_A^2 n^2 (k_B T)^3} \quad (4)$$

In Eq. (4), the surface energy γ has been replaced by an effective surface energy γ_{eff}, which , according to Hasson et al. (2003), is given by

$$\gamma_{eff} = \gamma \phi^{1/3} \quad (5)$$

where the parameter ϕ=1 for homogeneous nucleation and ϕ<1 (but usually unknown) for heterogeneous nucleation (Sohnel et al., 1987). For a given temperature, a plot of $\ln \tau_D$ vs. $(\ln S)^{-2}$ should yield a straight line, from the slope of which γ_{eff} can be determined.

RESULTS

Fouling in this system was measured thermally. The local heat transfer coefficient at a given thermocouple location along the length of the test section was determined from the following equation:

$$U = \frac{\dot{Q}}{(T_w - T_b)} \quad (6)$$

where $\dot{Q}$ was evaluated from the voltage and current applied to the test section, T_b from the linear relationship between the bulk inlet and outlet fluid temperatures as a function of thermocouple position, and T_w from the measured thermocouple temperature (T_o). The flow rate and hence velocity of the fluid through the TFU was measured using a calibrated rotameter. The reported bulk velocity is the time averaged value over the duration of the experiment.

For each experiment, the local heat transfer coefficient was measured by up to 10 thermocouples located at various axial positions. Figure 3 shows a plot of reciprocal local heat transfer coefficient (U^{-1}) versus time (TFU 703) for clean surface temperature $T_{w,c}$ = 82 °C, corresponding to the highest thermocouple (T_{10}). It consists of four different regions: a short heating up period (about half an hour), a nucleation delay time (horizontal region), a roughness control period in which the heat transfer enhancement of the scale roughness over-rides the heat transfer resistance of the scale, and a final region in which fouling over-rides scale roughness. Subtracting the heating up period time from the time where the horizontal line starts to decline determines the delay time for each thermocouple. This procedure was employed for all thermocouples that showed at least the start of a roughness control period.

In general, for each experiment the delay time decreases from T_1 (the lowest thermocouple on the test section) to T_{10} (the highest thermocouple), i.e. the top thermocouple (T_{10}) and the bottom one (T_1) showed the lowest and highest delay times, respectively, the delay time being a strong function of surface temperature. Thus, for example, in one experiment in which clean wall temperatures, $T_{w,c}$, at two different locations were 76°C and 82°C, respectively, the corresponding delay times, τ_D, were 14 hours and 6 hours. The results for experiments

Table 1. Delay time values for different operating conditions (V=1.2 m/s)

Run	703			707			706			708		
C(ppm)	3128			3291			3400			3600		
Location	$T_{w,c}(^\circ C)$	S	$\tau_D(hr)$	$T_{w,c}(^\circ C)$	S	$\tau_D(hr)$	$T_{w,c}(^\circ C)$	S	$\tau_D(hr)$	$T_{w,c}(^\circ C)$	S	$\tau_D(hr)$
T_1	73.3	1.29	13.73	73.1	1.35	7.36	72.4	1.40	4.71	73.2	1.48	1.28
T_2	74.5	1.29	13.92	73.8	1.36	5.93	73.7	1.41	4.17	73.8	1.49	1.09
T_3	75.1	1.30	13.73	75.1	1.37	5.39	74.2	1.41	3.08	74.5	1.50	0.91
T_4	76.5	1.31	12.08	76.4	1.38	5.39	76.4	1.43	2.17	75.9	1.51	0.72
T_5	77.5	1.32	8.61	77.2	1.39	4.13	78.1	1.43	2.17	76.6	1.52	0.54
T_6	78.2	1.33	9.34	78.7	1.40	2.87	78.5	1.44	2.17	78.3	1.53	0.54
T_7	79.2	1.33	6.77	79.2	1.40	2.87	80.3	1.45	2.17	78.8	1.54	0.36
T_8	80.6	1.34	9.33	81	1.41	1.61	81.1	1.46	1.27	80.9	1.55	0.36
T_9	81.7	1.35	8.60	81.2	1.42	1.61	81.5	1.46	1.27	81.1	1.55	0.36
T_{10}	82.1	1.35	6.04	81.8	1.42	1.61	82.2	1.47	0.72	81.7	1.55	0.36

Table 2. Surface energy values for different temperatures

	T_1	T_2	T_3	T_4	T_5	T_6	T_7	T_8	T_9	T_{10}
Location, Z (mm)	48	125	203	286	361	443	521	600	668	716
Temperature (°C)	73.0	74.0	74.7	76.3	77.4	78.4	79.4	80.9	81.4	82.0
$\gamma_{eff}\,(mJ/m^2)$	7.5	7.6	8.1	8.5	8.6	8.9	8.9	9.6	9.9	9.6

performed under different concentrations at a fixed velocity are presented in Table 1. Table 1 illustrates how delay time changes with concentration and surface temperature. It shows that delay time decreases with increases in both concentration and surface temperature. Also, based on the results in Table 1, a plot of $\ln \tau_D$ versus $(\ln S)^{-2}$ was constructed for each surface temperature. In Figure 4 the surface temperature is 82°C and the slope of the line determines the effective crystal surface energy, γ_{eff}, as 9.6 mJ/m^2. The effective surface energy values were calculated at other surface temperatures and the results are presented in Table 2. Surface energy values in Table 2 range from 7.5 to 9.9 mJ/m^2, mainly within the range 8-50 mJ/m^2, measured as surface energy for $CaSO_4 \cdot 2H_2O$ by several authors mainly in bulk precipitation. Also, for the surface nucleation, values of 7.9 and 14.6 mJ/m^2 have been reported by Linnikov (1999) for laminar flow on a metal surface and by Hasson et al. (2003) on a polymeric membrane surface, respectively.

For experiments performed at the same concentration and at a given velocity, plotting the logarithm of reciprocal delay time vs. the reciprocal of surface temperature, based on an Arrhenius equation (after Branch, 1991), determines the delay time activation energy at that velocity. Figure 5 is a delay time plot according to the equation

$$\ln(1/\tau_D) = \ln\Omega - E_D/RT_{w,c} \qquad (7)$$

for a given experiment, where individual thermocouple results were used to determine the surface temperature at a velocity of 0.5 m/s. Delay time activation energy E_D for this experiment was determined as 139 kJ/mol, and the pre-exponential factor Ω as 4.47 x 10^{16} s^{-1}. The results for all runs performed are presented in Table 3.

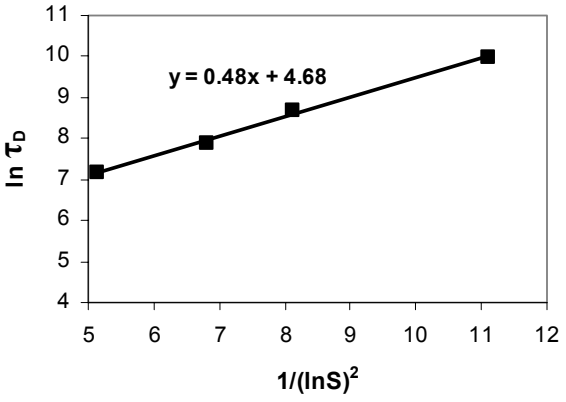

Figure 4. $\ln \tau_D$ vs. 1/(ln S)^2 (V = 1.2 m/s , $T_{w,c}$ = 82°C)

Table 3. Delay time activation energies for calcium sulfate experiments

C = 3400 ppm					
Run	**$T_{w,c}$ (°C)**	**T_b (°C)**	**V (m/s)**	**E_D (kJ/mol)**	**Ω (s^{-1})**
810	**63-83**	**51-59**	**0.15**	**79**	**5.99E+6**
811	**66-83**	**51-61**	**0.2**	**78**	**4.10E+7**
805	**71-83**	**51-62**	**0.3**	**119**	**6.21E+13**
804	**72-83**	**51-63**	**0.5**	**139**	**4.47E+16**
803	**72-83**	**51-63**	**0.7**	**163**	**1.94E+20**
806	**72-83**	**51-62**	**1.0**	**163**	**2.78E+20**
809	**73-82**	**51-62**	**1.2**	**163**	**2.30E+20**
807	**73-83**	**51-62**	**1.4**	**172**	**6.39E+21**
808	**73-83**	**51-62**	**1.6**	**165**	**4.22E+20**

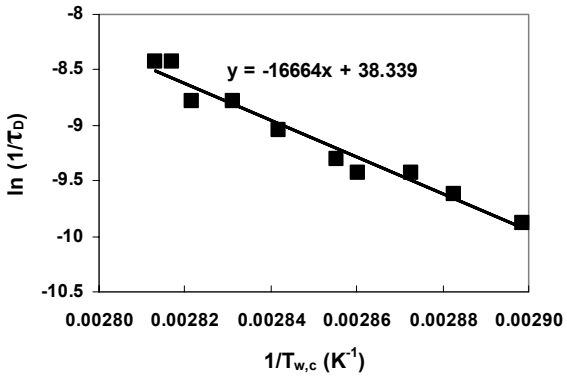

Figure 5. Delay time plot for TFU 804 (C=3400 ppm, V = 0.5 m/s)

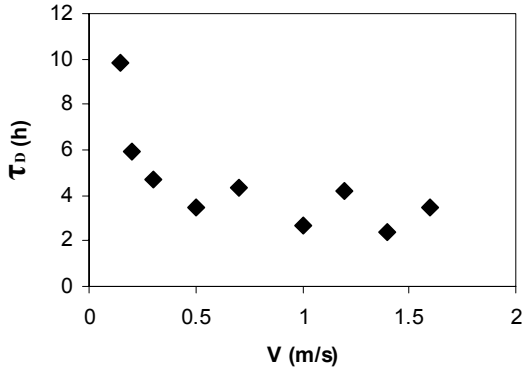

Figure 6. Effect of velocity on the delay time ($T_{w,c}$ = 82˚C, C = 3400 ppm)

Delay time activation energy values in Table 3 are higher than than the values of 50-72 kJ/mol measured for bulk precipitation of calcium sulfate by (Alimi et al. (2003). Figure 6 shows the effect of velocity on the delay time at a fixed clean wall temperature. It is seen that as the velocity increases, the delay time first decreases and then remains almost constant for velocities exceeding 0.5 m/s (which corresponds to Re =11200).

Figure 7 indicates how the delay time changes with bulk temperature at constant surface temperature. It is seen that as the bulk temperature increases the delay time decreases. At higher bulk temperatures the possibility of bulk precipitation, which contributes to particulate fouling, is higher and therefore delay time decreases.

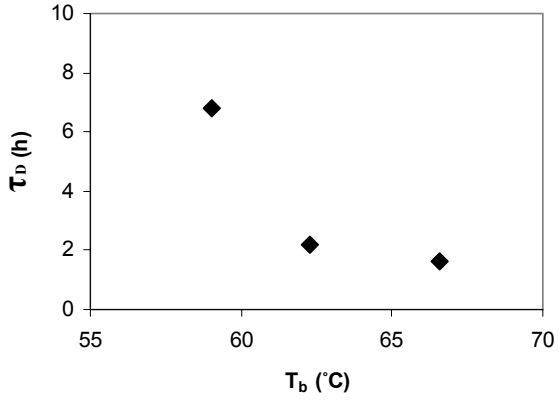

Figure 7. Effect of bulk temperature on the delay time ($T_{w,c}$ = 79˚C , C=3128 ppm, V= 1.2 m/s)

CONCLUSIONS

Calcium sulfate scaling delay time measurements under sensible heating conditions were carried out using a wall temperature measurement technique over a wide range of operating conditions. Delay time measurements were successfully correlated by a model based on nucleation theory and then calcium sulfate surface energy values were evaluated. Surface energy values for calcium sulfate nucleation measured in this study were in good agreement with other literature results. Also, delay time activation energy values were evaluated by plotting $\ln(1/\tau_D)$ versus $1/T_{w,c}$. The resulting delay time activation energy values were higher than those for bulk precipitation results from other researchers. Moreover, delay times were found to decrease not only with increasing surface temperature, but also with increasing bulk temperature and concentration. Finally, τ_D was found to decrease with increasing velocity up to a velocity of about 0.5 m/s and then remain almost constant at higher velocities.

ACKNOWLEDGMENTS

The authors are grateful to the Natural Sciences and Engineering Research Council of Canada for financial support.

NOMENCLATURE

A = frequency factor, $s^{-1}m^{-2}$
B =constant in Eq. (2), m^{-2}
C = solute concentration, ppm as $CaSO_4$
C_s = solute saturation concentration, ppm as $CaSO_4$
E_D = Delay time activation energy, J/mol
J = surface nucleation rate, $s^{-1}m^{-2}$
K = constant in Eq. (3), -
k_B = Boltzmann constant, 1.38 x 10^{-23} J/K
N_A = Avogadro's number, 6.022 x 10^{23} mol^{-1}
n = number of ions in a molecular unit
$\dot{Q}$ = heat flux, kW/m^2
R = universal gas constant, 0.008314 kJ/mol·K
S = supersaturation ratio, -
T = temperature, K
T_b = local bulk fluid temperature, ºC or K
T_o = local outside tube wall temperature, ºC or K
T_w = local inside tube wall temperature, ºC or K
t = time, s
U = local overall heat transfer coefficient, $kW/m^2 \cdot K$
V = bulk fluid velocity, m/s
Z = distance from lower cable connection (mm)
β = shape factor, $16\pi/3$
γ = crystal surface energy, $J.m^{-2}$
γ_{eff} = effective crystal surface energy, $J.m^{-2}$
τ_d = delay time, s or hr
v_m = molar volume, 7.445 E-5 m^3/mol
Ω = Delay time pre-exponential factor, s^{-1}
ϕ = nucleation correction factor, -

Subscripts

c = clean

REFERENCES

Alimi, F., Elfil, H., Gardi, A., "Kinetics of the Precipitation of Calcium Sulfate Dehydrate in a Desalination Unit," Desalination **157,** (2003), pp 9-16.

Branch, C. A. "Heat Transfer and Heat Transfer Fouling in Evaporators with Kraft Pulp Black Liquor," Ph.D. thesis, University of Auckland, New Zealand (1991).

Epstein, N., "Thinking about Heat Transfer Fouling: A 5 x 5 Matrix," Heat Transfer Engineering, **4**, (1983), pp.43-56.

Hasson, D., Drak, A., and Semiat, R., "Induction Times Induced in an RO System by Antiscalants Delaying $CaSO_4$ Precipitation," Desalination, **157,** (2003), pp 193-207.

Hasson, D., Drak, A., and Semiat, R., "Inception of $CaSO_4$ Scaling on RO Membranes at Various Water Recovery Levels," Desalination, **139,** (2001), pp 73-81.

Hasson, D., Zahavi, J., "Mechanism of Calcium Sulfate Deposition on Heat-Transfer Surfaces," I&EC Fundamentals **9,** (1970), pp. 1-10.

Linnikov, Oleg D., "Investigation of the Initial Period of Sulphate Scale Formation part 1. Kinetics and Mechanism of Calcium Sulphate Surface Nucleation at its Crystallization on a Heat-exchange Surface," Desalination, **122**, (1999), pp. 1-14.

Mullin, J. W., Crystallization, 4th ed., Butterworth-Heinemann., Oxford (2001).

Najibi, S. H., Muller-Steinhagen, H., Jamialahmadi, M., "Calcium Sulphate Scale Formation During Subcooled Flow Boiling," Chemical Engineering Science **52**, (1997), pp. 1265-83.

Rose, I. C., Watkinson, A.P., Epstein, N., "Testing a Mathematical Model for Initial Chemical Reaction Fouling using a Dilute Protein Solution," Canadian Journal of Chemical Engineering **78**, 5-11 (2000).

Sohnel, O, Mullin, J. W., "Interpretation of Crystallization Induction Periods," Journal of Colloid and Interface Science **123**, (1988), pp. 43-50.

Wilson, D.I., Watkinson, A. P., "A Study of Autoxidation Reaction Fouling Heat Exchangers," Canadian Journal of Chemical Engineering **74**, 236-246 (1996).